BioMedical Engineering OnLine

RESEARCH

Open Access

Muscle synergy and kinematic synergy analyses during sit-to-stand motions in hallux valgus patients before and after treatment with Kinesio taping

Ruiping Liu[1,3†], Yanyan Liu[2,3†], Lihua Zhou[1], Lei Qian[3], Chunyan Chen[3], Xinzhu Wan[3], Yining Wang[3], Wanqi Yu[3], Gang Liu[2*] and Jun Ouyang[3*]

†Ruiping Liu and Yanyan Liu have contributed equally to this work as co-first authors.

*Correspondence: lg2781@smu.edu.cn; jouyang@126.com

[1] Department of Anatomy, School of Medicine, Shenzhen Campus of Sun Yat-Sen University, Sun Yat-Sen University, Shenzhen, Guangdong, China
[2] Department of Rehabilitation Medicine, Nanfang Hospital, Southern Medical University, Guangzhou, Guangdong, China
[3] Guangdong Provincial Key Laboratory of Digital Medicine and Biomechanics and Guangdong Engineering Research Center for Translation of Medical 3D Printing Application and National Virtual and Reality Experimental Education Center for Medical Morphology (Southern Medical University) and National Experimental Education Demonstration Center for Basic Medical Sciences (Southern Medical University) and National Key Discipline of Human Anatomy, School of Basic Medical Sciences, Southern Medical University, Guangzhou, China

Abstract

Objectives: To explore the impact of hallux valgus (HV) on lower limb neuromuscular control strategies during the sit-to-stand (STS) movement, and to evaluate the effects of Kinesio taping (KT) intervention on these control strategies in HV patients.

Methods: We included 14 young healthy controls (HY), 13 patients in the HV group (HV), and 11 patients in the HV group (HVI) who underwent a Kinesio taping (KT) intervention during sit-to-stand (STS) motions. We extracted muscle and kinematic synergies from EMG and motion capture data using non-negative matrix factorization (NNMF). In addition, we calculated the center of pressure (COP) and ground reaction forces (GRF) to assess balance performance.

Results: There were no significant differences in the numbers of muscle and kinematic synergies between groups. In the HV group, knee flexors and ankle plantar flexors were abnormally activated, and muscle synergy D was differentiated. Muscle synergy D was not differentiated in the HVI group.

Conclusion: Abnormal activation of knee flexors and plantar flexors led to the differentiation of module D in HV patients, which can be used as an indicator of the progress of HV rehabilitation. KT intervention improved motor control mechanisms in HV patients.

Keywords: Hallux valgus, Kinematic synergy, Kinesio taping, Muscle synergy, Relationship, Sit-to-stand

Introduction

Hallux valgus (HV) is a bunion deformity with primary symptoms of foot pain and dysfunction [1]. In addition, the prevalence of HV is high, with an adult prevalence of 23% and a female prevalence of 2–15 times higher than that of males [2, 3]. As a result of foot pain and dysfunction, patients with HV may experience reduced quality of life, increased risk of falls, and even disability [4].

According to prior research, HV has been associated with decreased walking speeds and disruptions in activities of daily living [5, 6]. In addition, HV deformity leads to altered gait patterns and biomechanical characteristics of the hip, knee, and ankle joints, with increased hip internal rotation and knee abduction moments in patients with HV compared to healthy individuals [7–9]. Previous studies have focused on gait, but sit-to-stand (STS) movements in HV patients have not been studied in detail. From stable sitting to unstable standing, STS movements are an extremely important condition in determining muscle strength in the lower limbs of adults [10, 11], and the hip, knee, and ankle joints are important for performing STS. The position of the toe's changes body dynamics during STS movements [12]. Muscle disorders also greatly affect STS movements [13]. Moreover, it has been observed that HV diminishes short toe flexor strength in young women [14]. Consequently, HV patients may experience alterations in their neuromuscular control mechanisms during STS movements due to the modified biomechanical characteristics of the hip, knee, foot, and ankle. Further investigation into the neuromuscular control mechanisms during STS movements in HV patients is, therefore, warranted.

For the rehabilitation of HV, it is crucial to understand the underlying mechanisms of treatment to enhance therapeutic outcomes. Conservative treatments, particularly for mild cases of HV, are preferred and encompass a range of intervention such as orthotics, orthopedic insoles, oral medications, motion, and manipulation [15, 16]. Orthotics, for instance, target the first metatarsal by separating the first and second toes [17], while orthotic insoles mitigate first metatarsophalangeal joint deformities and stress by redistributing pressure in the toe area [18]. However, these methods are often hindered by their time-consuming application, patient discomfort, inconvenience, and limited utility. Conversely, Kinesio taping offers a promising alternative, effectively addressing pain, swelling, proprioception, and joint support, and enjoys widespread acceptance and applicability in clinical settings [19]. Short-term studies have demonstrated significant improvements in hallux valgus angle (HVA) following Kinesio taping intervention in HV patients [20], alongside enhanced gait stability and balance maintenance [21]. Nonetheless, the bulk of research on Kinesio taping focuses on its therapeutic and proprioceptive effects on muscles and joints [19, 22], leaving a gap in our understanding of its influence on motor control mechanisms in HV patients.

Musculoskeletal disorders can cause abnormalities in the neuromuscular system [23]. HV, as a common musculoskeletal system disorder, may also present with abnormalities in neuromuscular regulation. To investigate how the central nervous system (CNS) controls multiple muscles, Bernstein proposed the muscle synergy hypothesis, whereby instead of controlling the contraction of one muscle, the CNS controls motion by controlling the contraction of several groups of muscles [24, 25]. According to this hypothesis, the CNS can flexibly control the activation of a limited number of synergistic modules through the output of neural commands for a certain period to perform various daily activities [26–28]. Although the concept of synergy was originally used to describe intermuscular coordination, it has also been used to analyze the synergy of motions between joints (kinematic synergy) [29, 30]. Tagliabue et al. found that muscle synergy preceded kinematic synergy by one phase by investigating the correlation between muscle and kinematic synergism during two-finger grasping [31]. Over time, the CNS

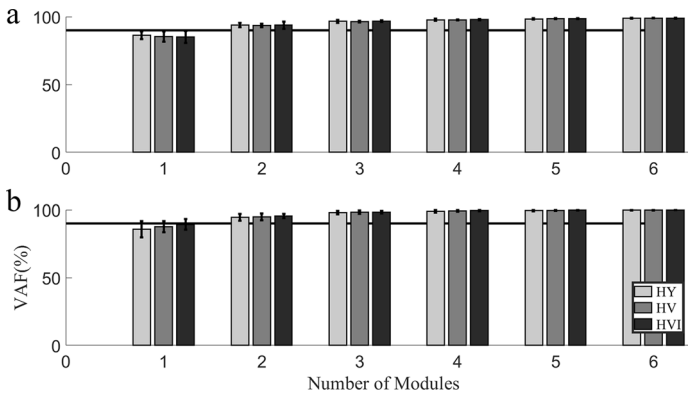

Fig. 1 Number of modules in each group. **a** Number of muscle modules selected by all subjects was 90% of the VAF. **b** Number of DOF modules selected by all subjects is 90% of VAF. (Left: HY group, middle: HV group, right: HVI group). The black horizontal line represents the threshold for the global VAF, which is set at 90%

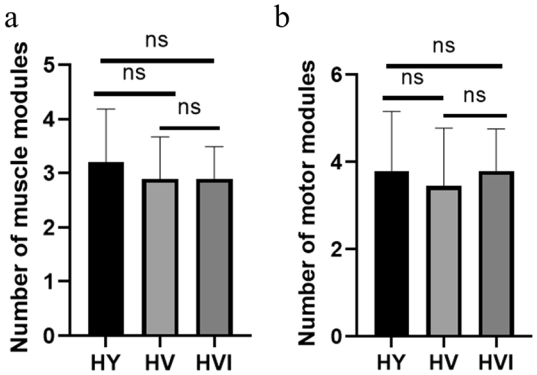

Fig. 2 **a** Number of muscle synergies in each group. **b** Number of kinematic synergies in each group. Bars indicate the mean and standard deviation for each data group. NS stands for no significant difference

flexibly controls kinematic synergy by controlling the recruitment of muscle synergy to complete walking [32]. However, the relationship between muscle synergy and kinematic synergy in STS tasks is unclear.

Therefore, our goal is to investigate the neuromuscular control strategy of HV during STS exercises and examine the changes in this strategy in HV patients before and after intervention. By doing so, we aim to gain a comprehensive understanding of the therapeutic effects of KT on HV patients. This study is expected to enhance our understanding of the motor control mechanisms involved in STS movement and improve the efficacy of physical therapy for HV patients.

Results

Number of muscle and kinematic modules

As far as muscle synergistic modules are concerned, 2–4 modules were extracted from the HY, HV, and HVI groups in the NNMF results (Fig. 1a). There were no statistically significant differences observed between the HY group and the HV group, nor between the HV group and the HVI group (Fig. 2a). For the kinematic synergy module, in the NNMF results, 2–5 modules were extracted in the HY, HV, and HVI groups (Fig. 1b).

There were no statistically significant differences observed between the HY group and the HV group, nor between the HV group and the HVI group (Fig. 2b).

Muscle synergies in each module

As shown in Fig. 3, in the HY group, the muscle synergies were denoted as HY-A, HY-B, HY-C, and HY-D. Similarly, in the HV group, they were labeled as HV-A, HV-B, HV-C, and HV-D. Finally, in the HVI group, they were identified as HVI-A, HVI-B, HVI-C, and HVI-D. The active muscles in the first module of the HY group (HY-A) include AH, EDL, EO, GL, PL, and TA, which serve to stabilize the ankle and assist in trunk forward flexion in phases 1 and 2. In the HY group, the muscles activated in the second module (HY-B) include the EDL, ES, GL, PL, TA, VL, VM, and RF. During phases 2 and early phase 3, these muscles collectively contribute to knee extension, ankle dorsiflexion, and spinal extension. The active muscles in Module 3 (HY-C) of the HY group include BF, EO, ES, GLM, SED, VL, VM, and RF, which serve to stretch the knee and hip joints and stabilize the ankle joint during the late second and third phases. Module 4 (HY-D): The active muscles of the HY group include EO, FHL, GL, SOL, GM, and SED. In the later phases of Phase 3 and Phase 4, the HY-D serves to assist in anterior trunk tilt, plantarflexion of the ankle, and flexion of the knee. Compared with the HY group, the HV groups showed some different characteristics. In the HV group, Module A (HV-A) lacked activation of TA and EDL, including activation of ES, SOL, GM, and FHL. The duration of HV-A was shortened in phases 1 and 2 and activated ankle plantarflexion and trunk stabilization effects in phase 4. The duration of module B (HV-B) increased in phase 1. Module C (HV-C) was additionally activated in phase 2. Module D (HV-D) including BF, ES, and PL was additionally activated, and the duration of phase 4 was shortened. Module A (HVI-A) of the HVI group does not include SOL activation compared to HV-A. The

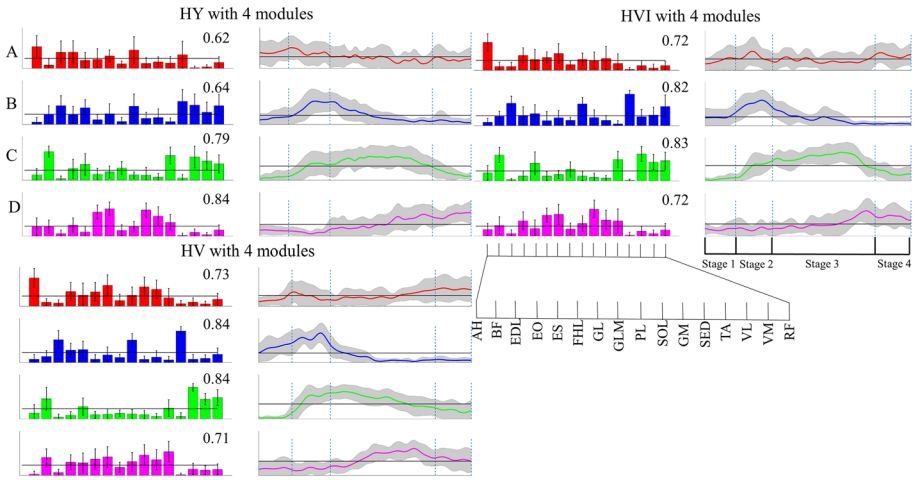

Fig. 3 Temporal and spatial patterns of all participants during the extraction of the four muscle synergy modules in each group. The four modules of muscle synergy are denoted by **A**, **B**, **C**, and **D**. For example, the first module of the three groups is labeled as HY-A, HV-A, and HVI-A, respectively. Each bar (left; histogram) and curve (right; line graph) represent the mean value for all participants in each group. Error bars (left; graph) and gray-scale plots (right; graph) represent the standard deviation. Each value (left; bar graph) represents the Pearson similarity in each module. The horizontal line (left panel) represents the threshold for the spatial component of the active muscle in the module. The horizontal line (right panel) represents the threshold for the temporal pattern of the module

duration of HVI-A is extended in phase 2. Module D (HVI-D) of the HVI group lacks ES activation compared to HV-D. The duration of HVI-A is extended in phase 2. Modules B and C of the HVI group (HVI-B, HVI-C) converge with the HY group.

Kinematic synergies for each module

As shown in Fig. 4, the kinematic synergies were HY-a, HY-b, HY-c, and HY-d for HY group, HV-a, HV-b, HV-c, and HV-d for HV group, and HVI-a, HVI-b, HVI-c, and HVI-d for HVI group. In the HY group, module a (HY-a) mainly includes A/DF, A/ADD, A/EVR, F/LPIT, H/FLX, and K/FLX.HY-a plays the roles of ankle dorsiflexion, adduction and valgus, foot left deviation, and hip and knee flexion in phases 1 and 2. Module b (HY-b) consists of A/DF, A/EVR, F/LPIT, K/FLX, H/FLX, and P/AO. HY-b is primarily used in late phase 2 and early phase 3 for ankle dorsiflexion and valgus, left foot valgus hip and knee flexion, and anterior pelvic tilt. Module c (HY-c) consists of A/DF, A/ADD, A/EVR, F/LPIT, H/ABD, and P/AO, which are mainly used in phase 3 for ankle dorsiflexion, adduction and valgus, left foot deviation, hip abduction, and anterior pelvic tilt. Module d (HY-d) consisted mainly of A/ADD, A/EVR, F/LPIT, and P/LO and played the roles of ankle dorsiflexion and valgus, foot left deviation, and pelvic left tilt at the end of phase 3 and phase 4. Compared with the HY group, the HV group's HV-c lacked ankle adduction (A/ADD) but increased hip and knee flexion (H/FLX, K/FLX). Compared with the HV group, the HVI group's HVI-c only increased hip flexion (H/FLX) and lacked hip abduction (H/ABD) and knee flexion (K/FLX).

Spatial composition of the synergy modules

Each value in Fig. 3 represents the average of the similarity of individual modules within a group. The similarity between groups was high (HY: 0.62–0.84; HV: 0.73–0.84; HVI: 0.72–0.83). As shown in Table 1, comparing the similarity between the four

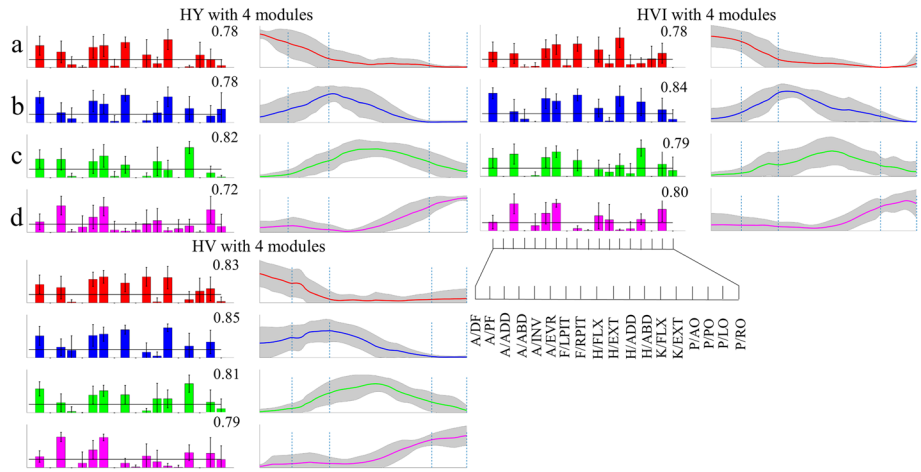

Fig. 4 Temporal and spatial patterns of all participants in each group during the extraction of the four kinematic synergy modules. The four modules of kinematic synergy are denoted by **a**, **b**, **c**, and **d**. For example, the first module of the three groups is, HY-a, HV-a, HVI-a, respectively. Each bar (left; histogram) and curve (right; line graph) represent the mean value for all participants in each group. Error bars (left panel) and gray-scale plots (right panel) represent standard deviations. Each value (left; bar graph) represents the Pearson similarity for each module. The horizontal line (left panel) represents the threshold for the spatial component of the DOF contained in the module

Table 1 Comparison of similarity of four muscle synergies between and within groups

Comparison of each module between groups			**Comparison of each module within groups**			
A	HY-A	HV-A	HY group	A	B	C
HV-A	0.46		B	0.08		
HVI-A		0.94***	C	− 0.65*	− 0.04	
B	HY-B	HV-B	D	0.00	− 0.56	− 0.26
HV-B	0.72**		HV group	A	B	C
HVI-B		0.91***	B	− 0.35		
C	HY-C	HV-C	C	− 0.38	− 0.45	
HV-C	0.81**		D	− 0.42	0.28	− 0.12
HVI-C		0.91***	HVI group	A	B	C
D	HY-D	HV-D	B	− 0.47		
HV-D	0.74**		C	− 0.29	− 0.33	
HVI-D		0.84***	D	− 0.50	0.41	− 0.28

The threshold value was set to 0.6. The values > 0.6 were defined as high similarity and < 0.6 as low similarity. * indicates $p < 0.05$, ** represents $p < 0.01$, *** represents $p < 0.005$

Table 2 Comparison of similarity of four kinematic synergies between and within groups

Comparison of each module between groups			**Comparison of each module within groups**			
a	HY-a	HV-a	HY group	a	b	c
HV-a	0.92***		b	**0.80****		
HVI-a		0.96***	c	0.43	**0.66****	
b	HY-b	HV-b	d	0.32	0.25	0.54*
HV-b	0.89***		HV group	a	b	c
HVI-b		0.94***	b	**0.80****		
c	HY-c	HV-c	c	0.50*	**0.75*****	
HV-c	0.94***		d	0.54*	0.43	0.57*
HVI-c		0.89***	HVI group	a	b	c
d	HY-d	HV-d	b	**0.84*****		
HV-d	0.92***		c	0.59**	**0.80****	
HVI-d		0.94***	d	0.46	0.40	**0.71****

The threshold value was set to 0.6. The values > 0.6 were defined as high similarity and < 0.6 as low similarity. In comparisons of between modules within each group (right), values in bold indicated higher than 0.6. * represents $p < 0.05$, ** represents $p < 0.01$, *** represents $p < 0.005$

modules within each group, the independence between the four modules within each group was high (Table 2, right). Comparing the similarity between the corresponding modules between groups, the similarity between the corresponding modules within each group was high, except for Module A (Table 2, left). In addition, we found that HY-D was also highly like HV-A ($r = 0.68$). As shown in Fig. 5, we found that HV-A and HV-D were differentiated from HY-D. HV-A and HV-D can reconstruct HY-D well ($r = 0.88$).

Each value in Fig. 4 represents the average of the similarity of each module within the group. The similarity between groups was high (HY: 0.78–0.82; HV: 0.79–0.85; HVI: 0.78–0.84). As shown in Table 2, comparing the similarity of the corresponding modules between groups, the similarity of the corresponding modules between

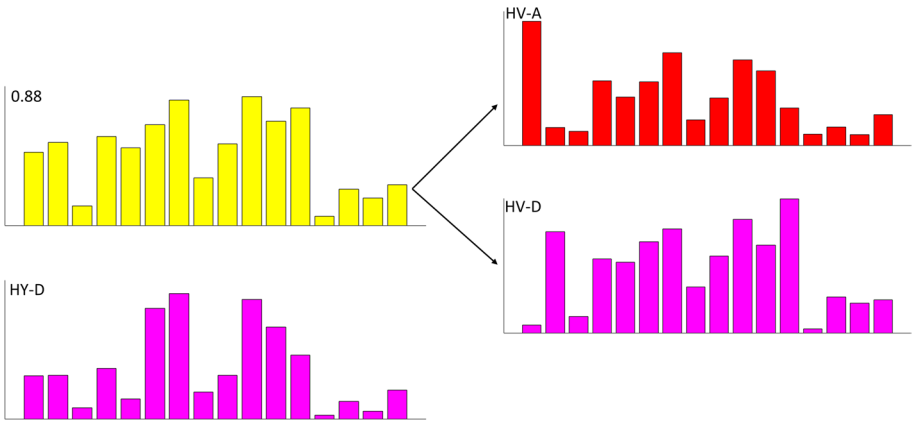

Fig. 5 Left leg muscle synergy in HV patients was interpreted as part of left leg muscle synergy in the HY group. Our computational procedure takes the synergies of HV-A and HV-D of the HV group to determine the fraction of synergies of HY-D of the HY group. Indeed, the muscle synergies (HV-A and HV-D) of the HV group identified as compartmentalized can be linearly combined to reconstruct the corresponding synergies of the uninvolved arm (yellow), which matches very well the synergies extracted from the HY group (HV-D) ($r = 0.88$)

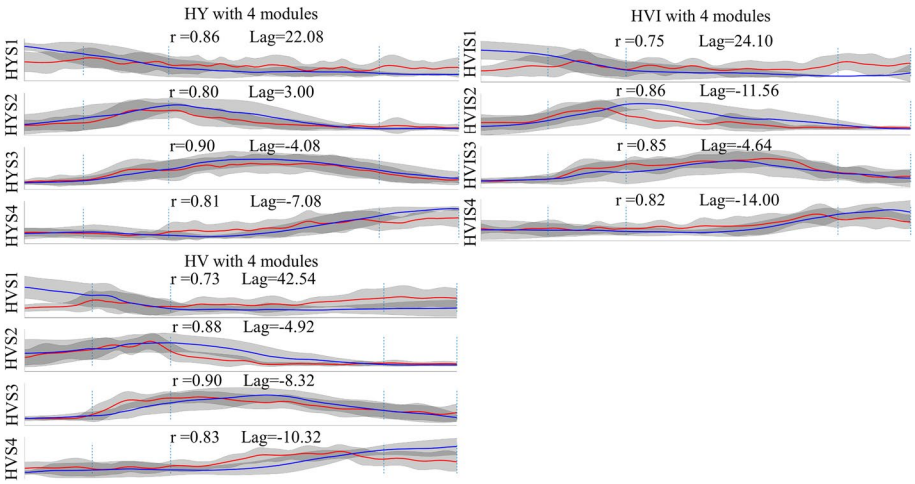

Fig. 6 Time-lagged cross-correlations of activation coefficients for muscle and kinematic synergies. The red and blue curves represent the temporal patterns of muscle synergy and kinematic synergy, respectively. The dotted line indicates the phase division of the motion cycle. In the HY group, all four modules (HYS1–HYS4, e.g., HYS1 denotes the activation coefficient of HY-A versus HY-a)

groups was high (a: 0.92–0.96; b: 0.89–0.94; c: 0.94–0.89; d: 0.92–0.94) (Table 2, left). Comparing the similarity of the four modules within each group, the independence between the four modules was low (Table 2, right). Among the four modules in the HY group, HY-a and HY-b and HY-b and HY-c were more similar. Among the four modules in the HV group, HV-a and HV-b and HV-b and HV-c were more similar. Among the four modules in the HVI group, HVI-a and HVI-b, HVI-b and HVI-c, and HVI-c and HVI-d were more similar.

Relationship between muscle and kinematic synergies

Figure 6 shows the close connection between the activation coefficients of muscle synergy and kinematic synergy in STS motion. In the HY group, all four modules (HYS1–HYS4, e.g., HYS1 denotes the activation coefficient of HY-A versus HY-a) showed high similarity (0.81–0.90). Where Lag < 0 indicates that muscle synergy is higher than kinematic synergy, Lag = 0 indicates that muscle synergy occurs simultaneously with kinematic synergy, and Lag > 0 indicates that muscle synergy lags kinematic synergy. In HYS1 and HYS2, kinesiology synergy superseded muscle synergy (Lag: 22.08–3.00). In HYS3 and HYS4, kinematic synergy lagged muscular synergy (Lag: −4.08 to −7.08). In the HV group, the similarity of the four modules (HVS1–HVS4) was also high (0.73–0.90). The correlation between muscle synergy and kinesiology synergy decreased in HVS1 compared to the HY group ($r = 0.73$). The correlation between muscle synergy and kinesiology synergy increased in HVS2 ($r = 0.88$), but kinesiology synergy lagged muscle synergy (Lag = −4.92). In the HVI group, the similarity between the four modules (HVIS1–HVIS4) was also higher (0.75–0.86), with an overall trend like that of the HV group.

Comparison between observational indicators

As shown in Fig. 7, the mean values of HVA and VAS in the HVI group were significantly lower than those in the HV group. As shown in Table 3, there were no significant differences in COP, vertical GRF, MT, and T-SO between the HV and HY groups. Similarly, there were no significant differences in COP, vertical GRF, MT, and T-SO between the HV and HVI groups.

Discussion

This study found no significant differences in the number of muscle synergies and motor synergies between the HY and HV groups or between the HV and HVI groups. These findings suggest that HV does not diminish the complexity of motor function in young individuals and that KT intervention does not alter the complexity of motor function in HV patients.

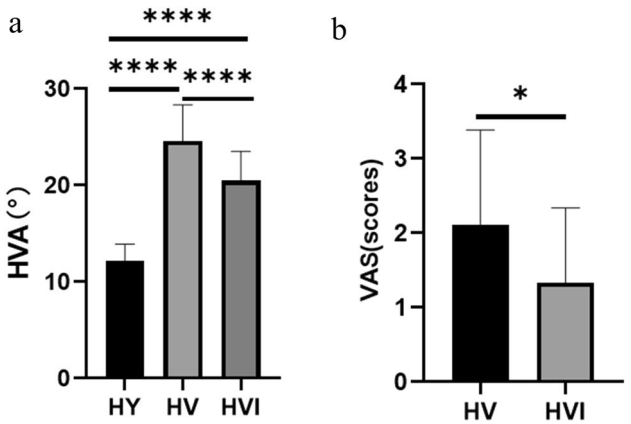

Fig. 7 **a** HVA in the three groups. **b** VAS in the HV and HVI groups. **** stands for $p < 0.001$.* stands for $p < 0.05$

Table 3 Comparison of observational indicators between groups

Group	HY	HV	HVI	*P1* value	*P2* value
COP-F	0.66 ± 0.02	0.71 ± 0.03	0.61 ± 0.02	0.568	0.056
COP-B	− 0.85 ± 0.36	− 1.03 ± 0.36	− 0.94 ± 0.22	1.484	1.65
COP-L	0.83 ± 0.20	0.70 ± 0.19	0.67 ± 0.30	1.332	1.882
COP-R	− 0.77 ± 0.21	− 1.29 ± 0.51	− 0.73 ± 0.26	0.596	0.522
COP-D	2.73 ± 0.28	2.59 ± 0.41	2.29 ± 0.22	1.562	0.89
GRF-Max	1.04 ± 0.02	1.07 ± 0.02	1.05 ± 0.03	0.732	0.694
MT (s)	1.55 ± 0.10	1.40 ± 0.07	1.45 ± 0.10	0.598	1.282
T-SO (s)	0.33 ± 0.02	0.35 ± 0.02	0.31 ± 0.01	0.82	0.204

Data are presented as mean ± SD. COP: center of pressure; GRF: ground reaction force; COP-F: average of COP displacement in the anterior direction; COP-B: average of COP displacement in the posterior direction; COP-L: average of COP displacement in the left direction; COP-R: average of COP displacement in the right direction; COP-D: total displacement of COP; GRF-Max: the peak of GRF; MT: motion time; T-SO: time of seat-off. *P1* value is statistical values for comparisons between the HY and HV groups. *P2* value is statistical values for comparisons between the HV and HVI groups

We further examined the similarity of muscle and motor synergies separately, as well as the spatial structure of each module. The results indicated that in the HV group, only the HV-A and HV-D modules could combine to form the HY-D module. This finding suggests that abnormal activation of plantar flexors and knee flexors is a marker of HV-related muscle activity. In addition, the spatial structure and activation timing of motor coordination were similar between the HY and HV groups, as well as between the HV and HVI groups. This implies that HV may not impair joint motor control and that KT intervention does not affect joint motor control in HV patients. Next, we explored the relationship between muscle synergy and kinematic synergy. The results showed a lagging relationship between kinematic synergy B and muscle synergy B in the HV groups compared with the HY group. The altered function of muscle synergy A in the HV groups led to delayed activation of muscle synergy A and earlier activation of muscle synergy B. This resulted in a decreased correlation between muscle synergy A and kinematic synergy A, and a lagged relationship between kinematic synergy B and muscle synergy B. These findings suggest that changes in muscle synergy function led to disruptions in muscle-kinematic synergy relationships, and short-term KT intervention do not improve these relationships.

Previous studies have found that diminished AH function in HV patient's results in insufficient effective pressure on the ground from the toes and reduced ankle balance [33]. The role of the FHL is to redistribute force from the rear foot to the front foot and enhance ankle balance [34]. HV increases in knee abduction moments [8]. In this study, HV-A in the HV group additionally activated the plantar flexors (FHL, SOL, and GM) as well as the muscles that maintain trunk stabilization (ES) and changed the activation time from phase 1 to phase 4. Additional activation of the knee flexors (BF), plantar flexors (PL), and muscles that maintain trunk stabilization (ES) was performed in HV-D. The activation time of HV-D is shifted forward. This strategic activation served to lower the body's center of gravity, stabilize the trunk and ankle joints, and enhance the effective pressure exerted by the foot on the ground. HV-A and HV-D in the HV group could be reconstructed by a linear combination of HY-D. Hence, the co-activation of the knee and ankle flexors and extensors during Phase 4 of the STS movement may not cause a significant shift in the COP for HV

patients. This differentiation in muscle synergy D production was only evident in the HV group. Our results showed no significant differences in the number of kinematic synergies between the HY and HV groups (Fig. 3). Analysis of the spatial structure of kinematic synergies revealed that HV-c in the HV group increased knee and hip flexion. This also reflects the fact that HV patients maintain balance in STS movements by flexing the knee and hip joints. The similarity analyses of kinematic synergistic spatial structures, as shown in Table 2, reveal that HV patients utilize similar motor modules to healthy young individuals during STS motion. Further analysis of MT, time away from sitting, COP, and GRF demonstrated that HV had little effect on lower extremity balance during STS movements, aligning with previous studies [9]. The altered relationship between muscle and kinematic synergy observed in the HV group may stem from changes in muscle synergy function. This adaptation may involve adjusting the activation coefficients of the four muscle synergy modules, compensating for changes in movement to ensure stable kinematic synergy. This emphasizes the sensitivity of muscle synergies in HV, where the CNS prioritizes the adjustment of muscle synergies to ensure the successful execution of STS movements. In conclusion, muscle synergism and the relationship between muscle synergism and kinematic synergism suggest a change in the pattern of neuromuscular control.

In this study, the HV group and the HY group, as well as the HV group and the HVI group, demonstrated a high degree of similarity in muscle synergies and corresponding kinematic synergies (Fig. 7), suggesting a direct correspondence between the two [32]. Notably, in the third and fourth modules, all groups demonstrated a lagging relationship between kinematic synergy and muscle synergy (Fig. 6). This implies that the achievement of the third and fourth kinematic synergies involved the recruitment of their corresponding muscle synergies. This observation aligns with earlier findings [32]. However, the results observed in the first module differ from previous studies. In this module, the muscle synergy of all three groups was noticeably lagging the kinematic synergy. The first kinematic synergy primarily encompasses the forward body lean and hip flexion observed during the initial phase of the STS movement. However, due to the limited number of trunk and hip muscle groups included in this study, the first muscle synergy may not fully capture all the muscle groups involved in forward body lean and hip flexion. As a result, the activation of the first muscle synergy may lag the activation of the first kinematic synergy. It's worth noting that among the muscles selected for this experiment, there are fewer muscles responsible for driving trunk and hip joint movements. However, kinematic synergy includes the movement of the hip joint and pelvis. This may lead to a significant lag in muscle synergy in module A compared to kinematic synergy in module a. In addition, the influence of joint position on muscle activation during joint movement may result in abnormal muscle activation [35], causing changes in the relationship between muscle synergy and kinematic synergy. These factors could explain the differences between our research results and previous studies. It is noteworthy that there was a lagged relationship between kinematic synergy and muscle synergy in the second module of the HV groups compared to the HY group. This may be due to the enhanced ankle dorsiflexion in the second muscle synergy in the HV group, which allowed the CNS to generate moments for STS movements by recruiting the second muscle synergy.

In conclusion, there is a one-to-one link between muscle synergism and kinematic synergism in the STS task, but the causal relationship between them may change as a function of muscle synergism.

Previous studies have found that KT improves muscle mobilization by shortening the distance between muscle origins and endpoints as well as by increasing receptor sensitivity, thereby improving motor unit recruitment [36]. The spatial structure similarity analysis of muscle synergies indicated a relatively low correspondence similarity of the four modules between the HV group and the HVI group (Table 2, left). Analysis of muscle synergy activation coefficients indicated an earlier onset and prolonged duration of module A during the second phase, as well as an extended duration of module D during the fourth phase in the HVI group. These findings suggest improved ankle and knee joint stability in HV patients during sit-to-stand motion following KT intervention. Analysis of the HVA and VAS showed that patients in the HVI group had reduced pain and a gradual return of the first metatarsophalangeal joint to its normal position. These results suggest that KT can correct HVA while reducing pain in patients with HV. Furthermore, existing literature indicates that KT treatment increases cutaneous sensory input [37] and enhances joint mobility [38] to alleviate pain. Thus, the central nervous system modulates the spatial structure of the A and D muscle modules, as well as the activation coefficients of the four muscle modules in HV patients. Our results indicated no significant differences in the number of kinematic synergies between the HV and HY groups or between the HV and HVI groups (Fig. 2b). However, we observed that the average number of kinematic synergies in the HVI group was closer to two. Spatial structure analysis revealed that the HVI group exhibited reduced knee flexion and hip abduction in the third stage. This suggests that hip and knee stability during the STS movement improved following KT intervention in the HV group. The spatial structure similarity analysis indicated that the kinematic cooperation module of the HVI group tended to consolidate into two kinematic cooperation modules. This consolidation may be attributed to the restrictions KT imposes on the foot joints of HV patients during the intervention. Consequently, the central nervous system of some HV patients appears to engage fewer and simpler kinematic coordination modules to enhance stability during STS movement. Our analysis of the relationship between muscle synergy and kinematic synergy demonstrated that short-term KT intervention did not improve the interaction between muscle and kinematic synergy in HV patients. Kinematic parameter analysis revealed no significant differences in MT, T-SO, COP, and vertical GRF between the HV and HVI groups. These findings suggest that KT may not disrupt homeostasis in HV patients during STS movement.

Notably, our study indicates that certain measurements, particularly in the TA group of HV and HY, exhibit high standard deviations. This variability stems from individual differences in muscle activity, joint flexibility, posture variations, and slight experimental condition variances. While this variability complicates data interpretation, we have employed robust statistical methods such as paired t tests and two-sample t tests to validate our conclusions. The substantial variability underscores the generalizability of our findings to real-world conditions. To mitigate high standard deviation in future research, we recommend augmenting sample sizes, refining

subgroup classifications, and enhancing measurement methodologies. These steps will minimize random and systematic errors, thereby improving data consistency and accuracy.

There are some limitations of this study. First, there was no velocity gradient set for the STS motion. The natural speed of the STS was used to ensure test uniformity for the participants as well as foot and ankle acceptance, and thus a high-speed STS test was not performed. Second, the small number of subjects may cause some of the data to be affected by individual differences resulting in large standard deviations. KT treatment was mainly applied to patients with mild-to-moderate HV, so all pain scores were low in this group of volunteers. Third, there was a gender imbalance. Because of the gender difference in the prevalence of HV, most participants in both the HV and HVI groups were female. Therefore, there is a need to increase the number of participants in future studies to determine the relationship between gender and HV and to improve this imbalance. Finally, regarding the limitations of the study design: we did not include a placebo control group, which may result in findings being influenced by uncontrolled factors, potentially impacting the validity of the conclusions. In future research, we plan to include a placebo control group to more accurately assess the true effects of Kinesio taping. The control group will receive non-functional taping, and all participants and researchers will be informed that it is an effective intervention, ensuring proper blinding.

Conclusion

During STS motion, muscle modules in individuals with HV exhibited divergence, attributable to abnormal activation of knee flexors and ankle plantar flexors. This observation implies that employing muscle synergy analysis may prove advantageous in future investigations of musculoskeletal disorders characterized by aberrant muscle activity components. Moreover, in the context of STS motions, HV does not exert a discernible impact on kinematic synergies and lower limb balance. However, it manifests in an altered relationship between muscle synergies and kinematic synergies. This suggests that compensatory mechanisms within muscle synergy may take precedence over those associated with kinematic synergy in the presence of HV. Notably, Kinesio Taping intervention may hold promise in restoring neuromuscular control among patients with HV, without introducing significant changes to kinematic synergy and lower limb balance. However, the high standard deviation observed in our study reflects significant variability arising from individual differences and changes in experimental conditions. Nevertheless, our primary conclusions remain robust and statistically significant. The presence of high standard deviation underscores the need for cautious generalization of our findings, considering individual variations. Future research should prioritize increasing sample sizes and refining subgroup classifications to mitigate standard deviation. These enhancements will enhance the reliability and applicability of our study outcomes.

Methods

Participants

This study recruited participants from the community through poster advertisements. A total of 14 healthy young individuals (HY) and 13 patients diagnosed with hallux valgus

Table 4 Characteristic analysis of participants

Group	Age (years)	Height (m)	Weight (kg)
HY (m/f = 7/7)	26.14 ± 2.47	1.68 ± 0.07	60.42 ± 10.18
HV (m/f = 10/3)	25.08 ± 2.17	1.65 ± 0.10	59.00 ± 12.81
HVI (m/f = 7/2)	24.73 ± 1.95	1.67 ± 0.10	59.54 ± 13.97

m/f, Proportion of males and females among the participants. Participants' basic information (age, weight, and height) is expressed as Mean ± SD

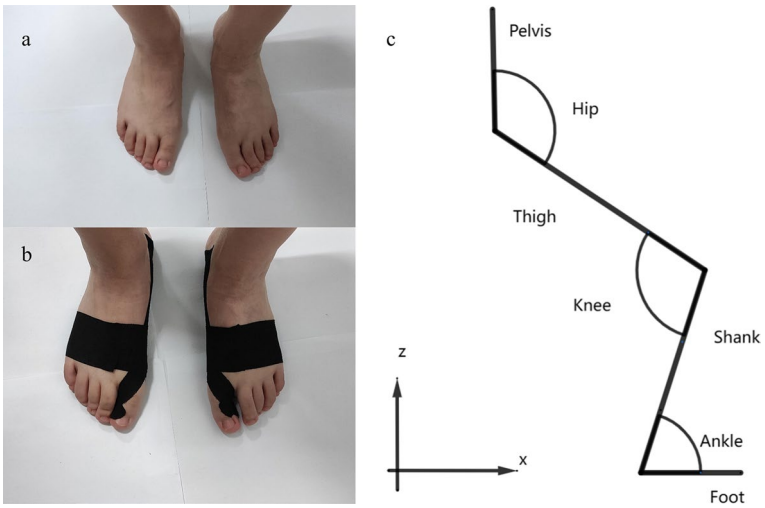

Fig. 8 **a** First metatarsophalangeal joint before the intervention in HV subjects. **b** First metatarsophalangeal joint in HV subjects' post-intervention. **c** Quadruple model from sitting to standing includes the pelvis, thighs, calves, and feet, as well as the hip, knee, and ankle joints

(HV) were enrolled. After completing initial assessments, the 13 HV patients underwent 1 month of Kinesio Taping (KT) treatment, during which new muscle patches were applied every two days. The same assessments were repeated after 1 month. Unfortunately, 9 HV patients (HVI) completed the intervention, as four dropped out due to personal reasons. Table 4 provides detailed demographic information. Motion data, including joint angles, center of pressure (COP), and ground reaction force (GRF), as well as hallux valgus angle (HVA), Visual Analog Scale (VAS) scores, and surface electromyography (EMG) readings, were collected [39, 40]. It's worth noting that all HV participants exhibited hallux valgus in both feet. HVA measurements were conducted by the same professional using a goniometer, with individuals having an HVA > 15° classified as having HV. Inclusion criteria comprised individuals aged between 18 and 44 years, right leg dominance, and the absence of any other musculoskeletal or neurological disorders.

Measurement experiment

All participants underwent three practice sessions prior to the formal testing to familiarize themselves with the test procedures. In addition, each participant was scheduled for testing at different time points to minimize the impact of practice effects on the study results. Participants were seated in a chair with no armrests and asked to complete 3 STS motions alone with their arms in front of their chest. HV patients treated with KT

were re-tested 1 month after the intervention. We processed the data for all subjects three times and calculated the mean of the three times for each subject as the final data for each subject. Mean as the final data for each subject. Figure 8a, b shows HV patients undergoing the intervention. A motion capture system (Miqus M1, Qualisys, Sweden; sampling frequency: 100 Hz) and two force measurement platforms (9260AA6, Kistler, Switzerland; sampling frequency: 1000 Hz) were used to acquire data for the calculation of joint angles (Fig. 8c), COP, and GRF. Joint angles included the left hip, left knee, and left ankle. To compute the motion trajectory of the joint angles, markers were pasted according to the CAST lower limb model [41], enabling the motion capture system to track the subject's motion trajectory by recognizing the position of the maker's marker motion.

A 16-channel surface electromyography (Mini Wave Infinity, Cometa, Italy; Sampling frequency: 2000 Hz) was used to acquire EMG signals. The measured muscles were defined as the 16 muscles of the left leg of all participants including erector spinae (ES), external oblique (EO), gluteus maximus (GLM), rectus femoris (RF), vastus medial (VM), vastus lateralis (VL), semitendinosus (SED), biceps femoris (BF), tibialis anterior (TA), peroneus longus (PL), extensor digitorum longus (EDL), gastrocnemius medialis (GM), gastrocnemius lateralis (GL), soleus (SOL), flexor hallucis longus (FHL), and abductor hallucis (AH). As depicted in Fig. 9, for precise muscle localization, two electrodes with a 1 cm radius were professionally affixed to the largest muscle belly of the corresponding muscles in the subjects by the same professional.

Data preprocessing

The following calculations were performed using MATLAB (version 9.0, R2016b, Mathworks Inc., Natick, MA). The raw EMG signal was filtered with a fifth-order high-pass Butterworth filter (50 Hz), demeaned, rectified, and then filtered with a fifth-order low-pass (5 Hz) Butterworth filter [23, 42]. The EMG data were normalized to the maximum value, ensuring equal weights, to obtain the EMG signal envelope matrix.

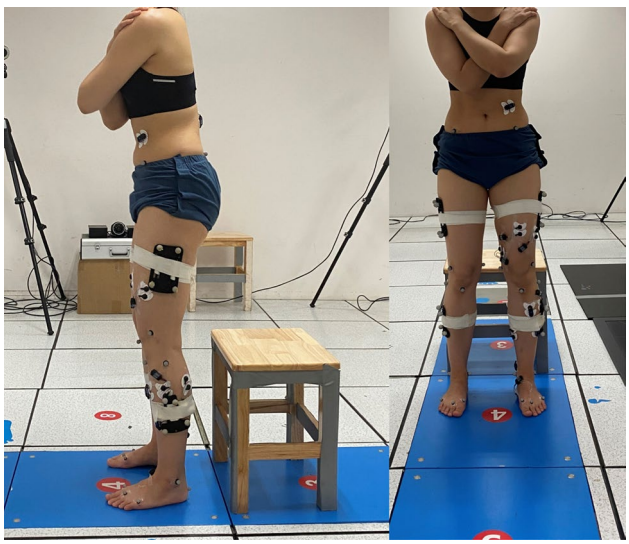

Fig. 9 Application of the motion markers and EMG electrodes

Kinematic and kinetic data were filtered with a sixth-order low-pass (10 Hz) Butterworth filter. Previous research has found that NNMF provides more physiologically meaningful results than other matrix factorization algorithms [43]. To extract kinematic synergies using NNMF, each joint angle is subdivided into two independent degrees of freedom with positive data values [44]. Therefore, half-wave rectification was used to decompose the joint angles. The joint angles were normalized to their maximum value, ensuring that their weights were equal, to obtain the kinematic degrees of freedom matrix. The kinematic degrees of freedom (DOF) were denoted as A/DF (ankle dorsiflexion), A/PF (ankle plantarflexion), A/ADD (ankle adduction), A/ABD (ankle abduction), A/INV (ankle inversion), A/EVR (ankle eversion), K/FLX (knee flexion), K/EXT (knee extension), H/FLX (hip flexion), H /EXT (hip extension), H/ADD (hip adduction), H/ABD (hip abduction), F/LPIT (foot left pitch), F/RPIT (foot right pitch), P/AO (anterior pelvic obliquity), P/PO (posterior pelvic obliquity), P/LO (left pelvic obliquity) and P/RO (right pelvic obliquity).

For the kinetic metrics, COP and vertical GRF peaks (GRF-Max) were obtained from the force platform and the total trajectory length (COP-D), left–right offset (COP-L, COP-R), and anteroposterior offset (COP-F, COP-B) were calculated. The left–right offset value is the distance on the y-axis from the center of the pressure trajectory relative to the center of the ankle joint, and the anteroposterior offset value is the distance on the x-axis from the center of the pressure trajectory relative to the center of the ankle joint. Finally, the total trajectory length, left–right offset, and anteroposterior offset were normalized using foot length. GRF-Max values were then normalized to the individual's body weight.

Based on the motion capture data and GRF, we divided the STS motion cycle into four phases [45]. In Fig. 10, we define the start of Phase 1 (Bend body) as the point at which the hip joint flexion angular velocity reaches 10% of its peak-to-peak value. The end of Phase 1 is marked when the derivative of the vertical ground reaction force (GRF) under the seat reaches 10% of its peak-to-peak value [46]. Phase 2 (Rise hip) begins when the derivative of the vertical GRF on the seat reaches 10% of its peak-to-peak value and ends when the vertical GRF on the seat reaches zero [47]. Phase 3 (Extend body) starts when the vertical GRF on the seat reaches zero and concludes when the horizontal displacement of the knee joint reaches its maximum. Phase 4 (Stabilization) begins when the horizontal displacement of the knee joint reaches its maximum and ends when the vertical GRF remains within 1% of body weight [47]. Subsequently, we standardize the

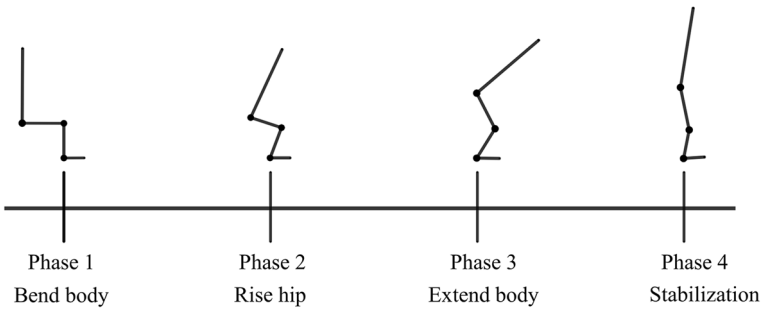

Fig. 10 Four phases of STS motion

duration of each phase as the average cycle duration of that phase across all subjects and trials. Based on these definitions, the movement time (MT) is calculated as the difference between the end time of Phase 4 and the start time of Phase 1."

Muscle synergies and extraction of kinematic synergies

To extract muscle and kinematic synergies, the EMG matrix or DOFs matrix was processed using NNMF. The above matrixes are represented as $n \times t$ matrix M, where n denotes the number of muscles and the number of kinematic DOFs, and t denotes the number of time points. The NNMF can be expressed as follows:

$$M = WH + E \tag{1}$$

where W denotes the spatial pattern of muscle synergies or kinematic synergies, H denotes the temporal pattern of muscle synergies or kinematic synergies, and E is the residual matrix. The spatial pattern, W, represents the relative activation level of the muscle or DOF, and the temporal pattern H represents the activation coefficient over time. To determine the number of muscle synergies or kinematic synergies, we calculated the variance accounted for VAF as follows [48]:

$$\mathrm{VAF} = 1 - \frac{||M - WH||}{||M||} \tag{2}$$

where VAF denotes the variance of the spatial–temporal modal reconstruction matrix in the original data matrix [49]. The number of muscle synergies necessary for interpreting sit-to-stand motion data was determined by selecting the minimum number of synergies that adequately reconstructed the muscle response. In this study, we employed two criteria to determine the optimal number of modules. First, all 16 muscles were required to have a Variance Accounted For (VAF) of $\geq 90\%$ [49]. Second, muscle synergies were also required to account for $> 75\%$ of the VAF in each muscle [50].

Similarity of muscle and kinematic synergies

For comparison, we extracted four modules from EMG data [51]. To explore the relationship between muscle synergies and kinematic synergies, we extracted four kinematic synergies from DOFs data. According to the principle of NNMF, a set of modules must be independent of each other. We used the Pearson correlation coefficient to measure the independence between the two modules. Pearson correlation coefficient is used to measure the degree of correlation between two vectors, when the value of two vectors is > 0.6, it means that there is a strong correlation between two vectors [51]. First, Pearson correlation coefficients were calculated for each individual's corresponding modules within each group to confirm the similarity of the modules across all members of the group. Next, we assessed the independence of the modules within each group. Finally, we compared the similarity of corresponding modules between the HY and HV groups, as well as between the HV and HVI groups. To determine the spatial structure of each module, the active muscles within a module were defined as those with a median value > 0.3 in the spatial pattern [52], and the active DOFs within a module was defined as the DOFs with a median value > 0.4 in the spatial pattern [31]. To determine that a

certain muscle synergy module was activated at the time, t, its activation coefficient, $h(t)$, is higher than the average activation coefficient $\overline{h(t)}$[53], given by the following equation:

$$\overline{h(t)} = \frac{\sum_{t_0}^{t_{\max}} h(t)}{t_{\max} - t_0} \tag{3}$$

After determining whether a particular module was activated or not, the chosen temporal characteristics were obtained as follows: (1) start time, the time of the first activation of this module; (2) end time, the time of the last activation of this module; and (3) duration: the length of the period between the start time and the end time.

In addition, muscle synergies may diverge. We systematically investigated this differentiation using a computational program that automatically linearly combined HV-A and HV-D to reconstruct HY-D. To assess the goodness-of-fit of the synergistic differentiation model, we computed the Pearson similarity between HY-D extracted from EMG signals and synergistic modules reconstructed from muscle synergism by merging muscle synergisms from the HV group.

The relationship of muscle and kinematic synergy

Time lag cross-correlation describes the degree of correlation between the values of the random signals $x(t)$ and $y(t)$ taken at any two different moments s, i, as per the following formula [54]:

$$R(s) = \frac{\sum_{t=-\infty}^{\infty} x(t)y(s+t)}{\sqrt{\sum_{t=-\infty}^{\infty} x(t)^2 \sum_{t=-\infty}^{\infty} y(t)^2}} \tag{4}$$

where $R(s)$ denotes the degree of correlation between the signals $x(t)$ and $y(t)$. Time lag cross-correlation can reflect the directionality between two signals, such as the lead–follow relationship, in which the lead signal initializes a response and the following signal repeats it. We used the time lag cross-correlation to analyze the relationship between muscle synergy and kinematic synergy.

Fractionation of muscle synergies

To determine the muscle synergy characteristics of HV patients, we initially assessed the similarity of the spatial structure of muscle synergy between the HY and HV groups. Our preliminary analysis revealed low similarity between HV-A and HY-A. Furthermore, paired comparisons of modules D and B between the two groups consistently showed the lowest similarity. Based on these findings, we hypothesized that module D might exhibit differentiation in the HV group. To further investigate, we modeled the muscle synergy in the HY group as a linear combination of multiple muscle synergies from the HV group. This approach aimed to examine whether multiple muscle synergies in the HV group could be considered components of the muscle synergy in the HY group. The coefficients for this linear combination were determined using a standard non-negative least squares procedure. To ensure a unique correspondence in the least squares optimization, we imposed additional constraints, specifying that each HV muscle synergy could contribute to the reconstruction of at most one HY muscle synergy.

Statistics

We utilized paired t tests to assess differences in Hallux Valgus Angle (HVA) and Visual Analog Scale (VAS) scores between the HV and HVI groups. In addition, differences in HVA between the Healthy Young (HY) and HV groups, as well as between the HY and HVI groups, were analyzed separately using two independent samples t tests. The number of muscle synergies and kinematic synergies were evaluated using the Mann–Whitney U test for comparisons between the HY and HV groups, and the HY and HVI groups. The HV and HVI groups were further analyzed using the Wilcoxon signed rank sum test. Parameters related to balance during STS motion, including Center of Pressure (COP) (COP-D, COP-F, COP-B, COP-L, and COP-R) and Maximum Ground Reaction Force (GRF-Max), were analyzed using paired samples t tests for the HV and HVI groups, and two independent samples t tests for the HY and HV groups. We employed the Bonferroni correction to account for the possibility of incorrectly rejecting a true null hypothesis, thereby minimizing the risk of such errors. A p value < 0.05 was considered statistically significant. All statistical analyses were performed using SPSS 20.0 (IBM, Armonk, New York, USA).

Author contributions

L.G. and OuY.J. designed the experiments. Q.L. and Z.L.H. provided the laboratory site and equipment. L.R.P. wrote the manuscript and data-processing programs, L.Y.Y. performed the analysis work, C.C.Y., and W.X.Z. collected the data, W.Y.N. and Y.W.Q. managed all volunteers. All authors approved the final version of the manuscript. There is no conflict of interest in this study.

Funding

This work was supported by the National Natural Science Foundation of China (No. 82274619, No. 32101054), the Natural Science Foundation of Guangdong Province (No. 2022A1515011681, No. 2021A1515010877), and the Basic and Applied Basic Research Project in Guangzhou (SL2023A04J01973).

Availability of data and materials

The data are not publicly available due to their containing information that could compromise the privacy of research participants.

Declarations

Ethics approval and consent to participate

The study was conducted by the Declaration of Helsinki and approved by the Institutional Ethics Committee of the Biomedical Ethics Committee of Southern Medical University (protocol code NFYKDX003). We explained the experiments in detail and obtained written consent from all participants.

Competing interests

The authors declare no competing interests.

Received: 16 February 2024 Accepted: 16 July 2024
Published online: 27 July 2024

References

1. Matsumoto T, Higuchi J, Maenohara Y, et al. The discrepancy between radiographically-assessed and self-recognized hallux valgus in a large population-based cohort. BMC Musculoskelet Disord. 2022;23(1):31.
2. Zhang WL, Zhao DY, Zhao W, Cui Y, Li Q, Zhang ZY. Effect of lentivirus-mediated miR-182 targeting FGF9 on hallux valgus. Int J Med Sci. 2021;18(4):902–10.
3. Ferreira GF, Stéfani KC. A global bibliometric analysis of hallux valgus Research (1999–2019). J Foot Ankle Surg. 2021;60(3):501–6.
4. Zeidan H, Ryo E, Suzuki Y, et al. Detailed analysis of the transverse arch of hallux valgus feet with and without pain using weightbearing ultrasound imaging and precise force sensors. PLoS ONE. 2020;15(1): e0226914.
5. Yoshida T, Tanino Y, Nakao T, Yamazaki W, Suzuki T. Examination of gait characteristics and related factors in elderly subjects with and without hallux valgus. Prog Rehabil Med. 2021;15(6):20210028.

6. Külünkoğlu BA, Akkubak Y, Çelik D, Alkan A. A comparison of the effectiveness of splinting, exercise and electrotherapy in women patients with hallux valgus: a randomized clinical trial. Foot (Edinb). 2021;48: 101828.
7. Chopra S, Moerenhout K, Crevoisier X. Characterization of gait in female patients with moderate to severe hallux valgus deformity. Clin Biomech. 2015;30(6):629–35.
8. Shih KS, Chien HL, Lu TW, Chang CF, Kuo CC. Gait changes in individuals with bilateral hallux valgus reduce first metatarsophalangeal loading but increase knee abductor moments. Gait Posture. 2014;40(1):38–42.
9. Nishimura A, Ito N, Nakazora S, Kato K, Ogura T, Sudo A. Does hallux valgus impair physical function? BMC Musculoskelet Disord. 2018;19(1):174.
10. Muñoz-Bermejo L, Adsuar JC, Mendoza-Muñoz M, et al. Test-retest reliability of five times sit to stand test (FTSST) in adults: a systematic review and meta-analysis. Biology. 2021;10(6):510.
11. Hyun SJ, Lee J, Lee BH. The effects of sit-to-stand training combined with real-time visual feedback on strength, balance, gait ability, and quality of life in patients with stroke: a randomized controlled trial. Int J Environ Res Public Health. 2021;18(22):12229.
12. Turcot K, Lachance B. How toe-out foot positioning influences body dynamics during a sit-to-stand task. Gait Posture. 2019;70:185–9.
13. Sütçü G, Yalçın Aİ, Ayvat E, et al. Electromyographic activity and kinematics of sit-to-stand in individuals with muscle disease. Neurol Sci. 2019;40(11):2311–8.
14. Yokozuka M, Okazaki K, Sakamoto Y, Takahashi K. Correlation between functional ability, toe flexor strength, and plantar pressure of hallux valgus in young female adults: a cross-sectional study. J Foot Ankle Res. 2020;13(1):44.
15. Macfarlane AJH, Kilmartin TE. Conservative treatment of juvenile hallux valgus - a seven-year prospective study. Br J Podiatry. 2004;7:101–5.
16. Hurn S, Smith M, Vicenzino B. A podiatry survey: How do we treat hallux valgus conservatively? J Foot Ankle Res. 2005;8:19.
17. Moulodi N, Kamyab M, Farzadi M. A comparison of the hallux valgus angle, range of motion, and patient satisfaction after use of dynamic and static orthoses. Foot. 2019;41:6–11.
18. Dissaneewate T, Na Rungsri T, Cheunchokasan P, Leelasamran W. Comparison between the plantar pressure effects of toe separators and insoles in patients with hallux valgus at a one-month follow-up. Foot Ankle Surg. 2022;28(1):93–9.
19. Dhein W, Wagner Neto ES, Miranda IF, Pinto AB, Moraes LR, Loss JF. Effects of Kinesio Taping on scapular kinematics and electromyographic activity in subjects with shoulder impingement syndrome. J Bodyw Mov Ther. 2020;24(2):109–17.
20. Żłobiński T, Stolecka-Warzecha A, Hartman-Petrycka M, Błońska-Fajfrowska B. The influence of short-term kinesiology taping on foot anthropometry and pain in patients suffering from hallux valgus. Medicina. 2021;57(4):313.
21. Akaras E, Guzel NA, Kafa N, Özdemir YA. The acute effects of two different rigid taping methods in patients with hallux valgus deformity. J Back Musculoskelet Rehabil. 2020;33(1):91–8.
22. Harput G, Guney H, Toprak U, Colakoglu F, Baltaci G. Acute effects of scapular Kinesio Taping® on shoulder rotator strength, ROM and acromiohumeral distance in asymptomatic overhead athletes. J Sports Med Phys Fitness. 2017;57(11):1479–85.
23. Kubota K, Hanawa H, Yokoyama M, et al. Usefulness of muscle synergy analysis in individuals with knee osteoarthritis during gait. IEEE Trans Neural Syst Rehabil Eng. 2021;29:239–48.
24. Donnally CJ, Patel PD, Canseco JA, et al. Current management of cervical spondylotic myelopathy. Clin Spine Surg. 2022;35(1):E68–76.
25. Shojaeefarda M, Khandana A, ArabBaniasada M, et al. O 027-There are common patterns of muscle synergy in cerebral palsy crouch gait. Gait Posture. 2018;65:55–6.
26. Cheung VCK, Cheung BMF, Zhang JH, et al. Plasticity of muscle synergies through fractionation and merging during development and training of human runners. Nat Commun. 2020;11(1):4356.
27. Hanawa H, Kubota K, Kokubun T, et al. Muscle synergies underlying sit-to-stand tasks in elderly people and their relationship with kinetic characteristics. J Electromyogr Kinesiol. 2017;37:15–20.
28. Mehryar P, Shourijeh MS, Rezaeian T, et al. Differences in muscle synergies between healthy subjects and transfemoral amputees during normal transient-state walking speed. Gait Posture. 2020;76:98–103.
29. Baniasad M, Farahmand F, Arazpour M, Zohoor H. Coordinated activities of trunk and upper extremity muscles during walker-assisted paraplegic gait: a synergy study. Hum Mov Sci. 2018;62:184–93.
30. Dewolf AH, Ivanenko Y, Zelik KE, Lacquaniti F, Willems PA. Kinematic patterns while walking on a slope at different speeds. J Appl Physiol. 2018;125(2):642–53.
31. Tagliabue M, Ciancio AL, Brochier T, Eskiizmirliler S, Maier MA. Differences between kinematic synergies and muscle synergies during two-digit grasping. Front Hum Neurosci. 2015;9:165.
32. Esmaeili S, Karami H, Baniasad M, Shojaeefard M, Farahmand F. The association between motor modules and movement primitives of gait: a muscle and kinematic synergy study. J Biomech. 2022;134: 110997.
33. Taş S, Çetin A. Mechanical properties and morphologic features of intrinsic foot muscles and plantar fascia in individuals with hallux valgus. Acta Orthop Traumatol Turc. 2019;53(4):282–6.
34. Kirane YM, Michelson JD, Sharkey NA. Evidence of isometric function of the flexor hallucis longus muscle in normal gait. J Biomech. 2008;41(9):1919–28.
35. Tsuruike M, Ellenbecker TS. Serratus anterior and lower trapezius muscle activities during multi-joint isotonic scapular exercises and isometric contractions. J Athl Train. 2015;50(2):199–210.
36. Christou EA. Patellar taping increases vastus medialis oblique activity in the presence of patellofemoral pain. J Electromyogr Kinesiol. 2004;14(4):495–504.
37. Halseth EK, McChesney C, Debeliso A, Vaughn J, Lienert DL. The effect of kinesio taping on proprioception and cutaneous stimulation in healthy adults: a review of the literature. J Athl Train. 2004;39(3):278–84.
38. Merolla G, Archini E, Paladini G, Cervellati G, Porcellini G. The use of kinesio tape for the treatment of shoulder pain and mobility in the early phases of rehabilitation after surgery: a randomized clinical trial. J Shoulder Elbow Surg. 2010;19(4):628–35.

39. Knörr J, Soldado F, Violas P, Sánchez M, Doménech P, de Gauzy JS. Treatment of hallux valgus in children and adolescents. Orthop Traumatol Surg Res. 2022;108(1S): 103168.
40. Sutton RM, McDonald EL, Shakked RJ, Fuchs D, Raikin SM. Determination of minimum clinically important difference (MCID) in visual analog scale (VAS) pain and foot and ankle ability measure (FAAM) scores after hallux valgus surgery. Foot Ankle Int. 2019;40(6):687–93.
41. Leardini A, Sawacha Z, Paolini G, Ingrosso S, Nativo R, Benedetti MG. A new anatomically based protocol for gait analysis in children. Gait Posture. 2007;26(4):560–71.
42. Cheung VC, Turolla A, Agostini M, et al. Muscle synergy patterns as physiological markers of motor cortical damage. Proc Natl Acad Sci USA. 2012;109(36):14652–6.
43. Lambert-Shirzad N, Van der Loos HF. On identifying kinematic and muscle synergies: a comparison of matrix factorization methods using experimental data from the healthy population. J Neurophysiol. 2017;117(1):290–302.
44. Baniasad M, Baghdadi S, Farahmand F, et al. Kinematic synergies are recognizable in the walker-assisted gait of spinal cord injury patients. Gait Posture. 2019;73:207–8.
45. Yoshida K, An Q, Hamada H, Yamakawa H, Tamura Y, Yamashita A, Asama H. Artificial neural network that modifies muscle activity in sit-to-stand motion using sensory input. Adv Robot. 2021;35(13–14):858–66.
46. Bahrami F, Riener R, Jabedar-Maralani P, Schmidt G. Biomechanical analysis of sit-to-stand transfer in healthy and paraplegic subjects. Clin Biomech. 2000;15(2):123–33.
47. Cameron DM, Bohannon RW, Garrett GE, Owen SV, Cameron DA. Physical impairments related to kinetic energy during sit-to-stand and curb-climbing following stroke. Clin Biomech. 2003;18(4):332–40.
48. Israely S, Leisman G, Machluf CC, Carmeli E. Muscle synergies control during hand-reaching tasks in multiple directions post-stroke. Front Comput Neurosci. 2018;12:10.
49. Gui K, Zhang D. Influence of locomotion speed on biomechanical subtask and muscle synergy. J Electromyogr Kinesiol. 2016;30:209–15.
50. Chvatal SA, Ting LH. Voluntary and reactive recruitment of locomotor muscle synergies during perturbed walking. J Neurosci. 2012;32(35):12237–50.
51. Zhenshuo LEI, Songtao LIU, Yang GE, et al. High conflict evidence fusion method based on average evidence and focal element distance. Electro-Optic Control. 2021;28:6–10.
52. Xiong QL, Wu XY, Yao J, et al. Inter-limb muscle synergies and kinematic analysis of hands-and-knees crawling in typically developing infants and infants with developmental delay. Front Neurol. 2018;9:869.
53. Yang N, An Q, Kogami H, et al. Temporal features of muscle synergies in sit-to-stand motion reflect the motor impairment of post-stroke patients. IEEE Trans Neural Syst Rehabil Eng. 2019;27(10):2118–27.
54. El-Gohary M, McNames J. Establishing causality with whitened cross-correlation analysis. IEEE Trans Biomed Eng. 2007;54(12):2214–22.

Publisher's Note